J Therm Spray Tech (2017) 26:970–984
DOI 10.1007/s11666-017-0557-2

PEER REVIEWED

Numerical Simulations of the High-Velocity Impact of a Single Polymer Particle During Cold-Spray Deposition

Sagar Shah[1] · Jonghyun Lee[1] · Jonathan P. Rothstein[1]

Submitted: 6 March 2017 / Published online: 24 April 2017

Abstract In this paper, deposition of polymer powders was studied numerically for the cold-spray deposition technique. In cold spray, a solid particle is impacted on a substrate at high velocity. The deformation and heating upon impact have been shown to be enough to result in particle deposition and adhesion even without melting the particle. Here, a systematic analysis of a single high-density polyethylene particle impacting a semi-infinite high-density polyethylene substrate was carried out for initial velocities ranging between 150 and 250 m/s using the finite element analysis software ABAQUS Explicit. A series of numerical simulations were performed to study the effect of a number of key parameters on the particle impact dynamics. These key parameters include particle impact velocity, particle temperature, particle diameter, composition of the polyethylene particle, surface composition and the thickness of a polyethylene film on a hard metal substrate. The effect of these parameter variations on the particle impact dynamics were quantified by tracking the particle temperature, deformation, plastic strain and rebound kinetic energy. The trends observed through variation of these parameters provided physical insight into the experimentally observed window of deposition where cold-sprayed particles are mostly likely to adhere to a substrate.

Keywords ABAQUS Explicit · finite element analysis · high-density polyethylene · high-velocity particle impact

✉ Jonghyun Lee
jonghyunlee@ecs.umass.edu

[1] University of Massachusetts, Amherst, MA 01003, USA

Introduction

The high-speed impact of small particles on a substrate can yield a variety of results depending on the particle velocity, impact angle, the size and shape of the particle and the particle and substrate materials involved. The possible outcomes include peening or permanent indentation of the substrate, erosion from the substrate, substrate abrasion, adhesion of particle to the substrate or material loss due to damage (Ref 1, 2). Depending on the type of process and desired outcome, these effects can be considered detrimental or beneficial. Due to the recent advances and commercialization of a number of different additive manufacturing processes, a large number of experimental, numerical and theoretical studies have been conducted to understand the impact process. Of particular interest here is the process known as cold spray where metal particles are accelerated to very high speeds and impacted onto a metal substrate where they deform and adhere all the while remaining in the solid state. The cold-spray process has become popular in the aerospace and other industries as a mechanism for repair and reconditioning of metal parts (Ref 3). Although, with new advances, this technique is finding other useful applications. When a solid metal particle impacts on metal substrate with sufficient kinetic energy, large deformation of the substrate may lead to an adiabatic shear instability and the formation of a 'jet' at the deformed interface between the particle and the substrate. This is because as the impacted particle deforms, the temperature at the interface will increase rapidly due to frictional heating and extremely short timescale of the impact. If the material softens at a higher rate compared to its rate of strain hardening, it starts to flow and forms a jet (Ref 4-6). The timescale for high-speed particle impact is of the order of a few hundred nanoseconds depending on the particle material and the impact velocity. Unfortunately, this is currently too short to be effectively examined by experiments. Therefore, there is a need to study the cold-spray impact process through numerical simulations. A number of research groups have been developing numerical models to address the phenomena during metal particle impact for last decades. Recently, in numerical analysis conducted by Yildirim et al. (Ref 1), the impact of a copper particle on a copper substrate for the velocities ranging between 100 and 700 m/s was studied. The use of the Lagrangian approach (with and without material damage) and the arbitrary Lagrangian–Eulerian (ALE) approach were investigated, and the Lagrangian approach with material failure was found most effective in describing the material behavior under high deformation and preventing excessive distortion of the mesh. The Lagrangian approach with material damage also allowed a more realistic prediction of the deformed shape of an impacted particle. A notable similarity in deformation patterns was observed between impacts of 50 μm and 5 mm particles as smaller particles were found to behave slightly stiffer than larger particles because of strain-rate effects.

Li et al. (Ref 7) studied the mesh dependence and the effect of particle size along with the use of material damage. The results showed that the simulations with material damage cope well with the element excessive deformation, and the resultant output is more reasonable than that obtained without material damage. The meshing size was found to have little effect on the output; also the particle size had very little effect on the morphologies of the deformed particles. Zhou et al. (Ref 8) considered the effect of initial temperature of the particle and substrate and the particle velocity on the deposition coating. It was found that as the in-flight temperature of the particle was increased, the coating became denser and microhardness and bond strength for metallic particles increased. The particle velocity and temperature need to be within a defined limit for adhesion to take place; the impact may result in fracture of the particle upon impact for low temperatures and velocities; however, the particle will deform excessively for high velocities and temperatures. Later, Zhou established that the initial kinetic energy of the particle was the dominant factor in deposition, and thus, the effect of initial temperature was not considered.

In this study, we will concentrate not on metal cold spray, which is a well-studied topic, but on a novel cold-spray process that utilizes polymer powders (Ref 9-12). The impact of polymer powders differs significantly from that of metals (Ref 12). As a result, much is unknown, including what is a suitable range for the particle velocity and can the rule of thumb settings used in metal cold sprays be applied to polymer particles. Too small velocities would not cause sufficient deformation or heating in the particle to ensure adhesion. On the other end, extreme velocities would induce large stresses on the target, large enough to overcome adhesion and strip the particles right off the substrate (Ref 13). Our approach is to study the impact numerically which in conjunction with experiments can help define a window of deposition and help physically understand the experimental results.

In order to properly simulate the high-speed impact of cold-spray process, polymer material properties at high strain rates must be determined. Although the literature is sparse in this area, efforts of Xu and Hutchings (Ref 12) and Bush et al. (Ref 9) give interesting insights on the polymer particle behavior. The results suggest that impact velocities between 100 and 200 m/s are necessary to deposit polymer particles on a polymer substrate. This informed our choice of initial velocity of 200 m/s for a 50-μm particle in the current study. Although significant melting was not observed during impact, some thermal effects might occur aiding interdiffusion and bonding between the plastically deformed particle and the substrate. Deposition onto hard aluminum substrates proved difficult for almost all spray conditions; heating the aluminum substrate gave good deposition though. The initiation of the deposition on a hard aluminum substrate represented a critical step, thus requiring a thin melted layer of polymer on the aluminum substrate before the low-temperature impact deposition occurred. Ravi et al. (Ref 10) successfully cold-sprayed ultra-high molecular weight polyethylene-nano-ceramic composite on polypropylene and aluminum. Working from these advances, it is now possible to model the high-speed impact of polymeric particles on hard and soft substrate and better understand the conditions under which adhesion is possible (Ref 12).

In this study, the von Mises plasticity model with temperature and strain-rate dependence was used. The first part of the study describes in detail the formulation of the finite element code and the various model parameters that were integrated into the code. In the second part of the paper, a parametric study investigating the effect of various physical properties and process parameters that have on the mechanics of particle deformation is conducted. The parameters studied include the impact velocity, the initial particle temperature, the particle diameter, the relative hardness between the particle and substrate material and the thickness of an already deposited layer of polymer material. Finally, we draw conclusions from our data and relate the results back to the experimental results in polymeric cold spray.

Numerical Methods

Simulation Properties

The single particle impact for polymers and the deformation characteristics were studied using the commercially available finite element analysis software ABAQUS/Explicit version 6.14 (Ref 14). The Lagrangian approach was adopted to simulate the particle impact (Ref 1). A 3D model with quarter symmetry was generated; due to lack of available material constants for the damage model, simulations were carried without the damage model. A 3D model was utilized rather than an axisymmetric model so that simulations of multiple particle impacts could be more easily performed in the future. The particle and the substrate were set to room temperature ($T_i = 298$ K) and were kept constant for all the cases except when studying the effect of temperature. The particle diameter was set to $D = 50$ µm for all simulations except when the effect of particle diameter was studied. Initial particle velocities between $U_\mathrm{i} = 150$ and 250 m/s were investigated by assigning the initial velocity to all the nodes of the particle. In order to ensure that the reflecting waves from the bottom face and the far off faces of the substrate reach the impact zone only after rebound of the particle and thus have no effect on the rebound characteristics of particle, the substrate was modeled as a cylinder with radius and height 25 times larger than the particle radius. The bottom face of the substrate was fixed in all degrees of freedom, while symmetric boundary conditions were applied on the vertical faces such that they were allowed to move only in the *y*-direction as defined in Fig. 1(a).

A fully coupled thermal stress analysis was conducted with eight-node reduced integration elements (C3D8RT) which have both temperature and displacement degrees of freedom. The effects of gravity were neglected. General contact algorithm with the friction coefficient of 0.3 was used for all the cases studied here.

Before discretizing the domain, mesh resolution dependence was investigated by varying the number of elements along the particle diameter from 50 elements to 200 elements. The mesh distribution was regular; no convergence expression was employed during the study. The mesh was fixed by selecting a value (ranging from 50 elements to 200 elements) for the number of elements along the particle diameter at the start of the simulation and was kept consistent throughout the simulation. This convergence study was performed to strike a balance between the mesh density and the improvement in the result by manually varying the mesh density of the entire domain before the start of the simulation. The results improved when the mesh size was changed from 50 elements to 100 elements, but further increase in the number of elements just added to the computation time without any further improvement in the results. Therefore, mesh density of 100 elements along the particle diameter was used for all the cases. To ensure better convergence, the element sizes at the particle substrate interface were kept the same. For computational efficiency, the mesh density was reduced two particle diameters away from the impact area in the substrate as shown in Fig. 1(b).

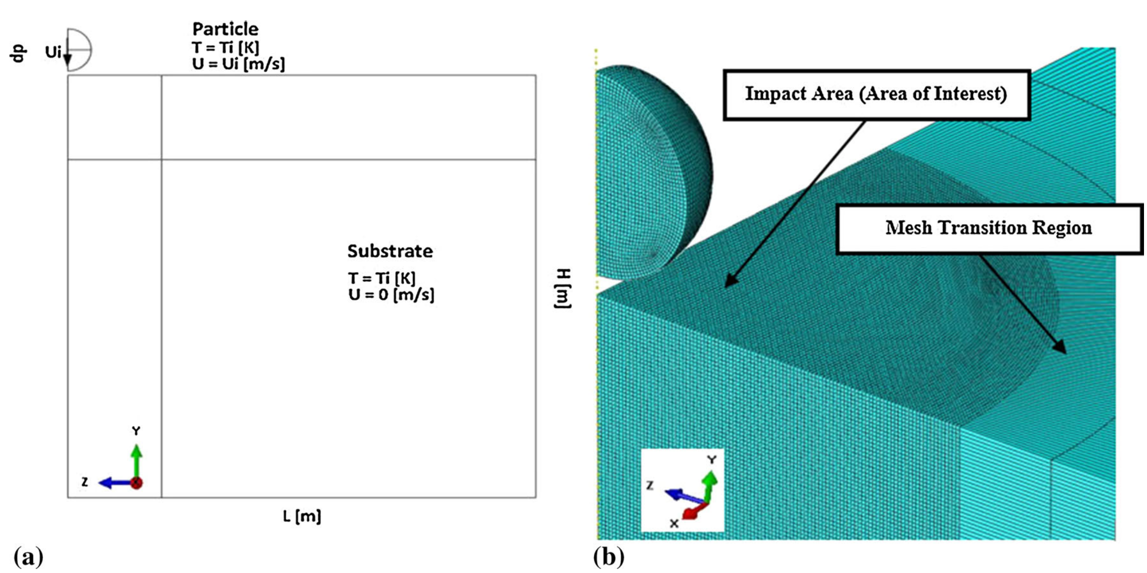

Fig. 1 (a) Initial conditions used for the impact of high-density polyethylene particle on substrate are shown, and (b) computational domain showing the mesh used in simulations (mesh resolution of 1/50*D* for a 50 µm particle) is shown

Material Model

General Properties

The elastic response of the material was assumed to be linear and defined by the elastic modulus and the Poisson's ratio. Thermal response was described by the specific heat and thermal conductivity. Material properties for elastic and thermal response at room temperature are shown in Table 1 (Ref 15).

Plasticity Model

The plastic deformation in the material was modeled by using isotropic material hardening. The flow stress of the material was modeled by the von Mises plasticity model (Ref 16). This model interprets yielding as a purely shear deformation process which occurs when the effective shear stress σ_e reaches a critical value. This effective stress is defined in terms of the principal stresses σ_i ($i = 1$, 2 or 3) by

$$\sigma_e = \left\{\frac{1}{2}\left[(\sigma_1 - \sigma_2)^2 + (\sigma_2 - \sigma_3)^2 + (\sigma_3 - \sigma_1)^2\right]\right\}^{1/2}. \quad \text{(Eq 1)}$$

The von Mises criterion then relates σ_e to the yield stress in tension σ_T by

$$\sigma_e = \sigma_T. \quad \text{(Eq 2)}$$

This criterion predicts that the tensile yield stress σ_T, effective shear yield stress σ_S and compressive yield stress σ_C are related by

$$\sigma_T = \sigma_c = \sqrt{3}\sigma_S. \quad \text{(Eq 3)}$$

High-density polyethylene was used as both particle and substrate material in most cases. Other cases for the parametric study used polycarbonate (PC), low-density polyethylene (LDPE) and oxygen-free high conductivity (OFHC) copper along with high-density polyethylene (HDPE). The effect of strain and strain-rate hardening, and thermal softening are shown in Fig. 2 as stress versus strain plots for HDPE at various strain rates and temperatures (Ref 17). Additional data for PC, LDPE and OFHC copper can be found in Ref 1, 17, 18. These data points were entered into ABAQUS as temperature and strain-rate-dependent data.

As shown in Eq 3, the classic von Mises elastic plastic model relates the effective stress to yield stress in tension. However, studies have shown that when considering additional stress states such as shear and compression simultaneously, yielding can be sensitive to the hydrostatic component of stress in addition to the shear component (Ref 16). Because the von Mises criterion does not consider hydrostatic stress, one will expect a slight loss in accuracy in the prediction of particle deformation. However, even if not fully quantitative, the von Mises model is known to give satisfactory insight into how parameter variation can affect the deformation mechanics and is used in impact dynamic simulations (Ref 14).

Table 1 Other material properties for high-density polyethylene

Properties	Value	Unit
Density(a)	960	kg/m^3
Elastic modulus(a)	0.7	GPa
Poisson's ratio(a)	0.42	
Thermal conductivity(a)	0.47	W/mK
Inelastic heat fraction	0.9	
Specific heat(a)	1900	J/kg K

(a) Temperature-dependent properties

Results and Discussion

A series of numerical simulations were performed in order to study how a number of key parameters affect the particle impact dynamics and the ability of the particle to adhere to the substrate. These parameters include particle temperature, particle size, particle impact velocity, composition of the polymer particle, surface composition and the thickness of a polymer film on a hard metal substrate. The effect of parameter variation on impact dynamics was quantified by tracking particle temperature, deformation, plastic strain, rebound velocity and kinetic energy, and the compression ratio of the particle.

Effect of Particle Temperature

The final temperature of a metal particle after impact largely depends on the initial velocity and initial temperature. In the case of polymer particles, a large temperature spike on impact can induce local melting and polymer chain interaction and entanglement between the particle and substrate that can greatly enhance adhesion which cannot be achieved by van der Vaals forces alone (Ref 19). The temperature of the polymer particle will also affect how the material behaves during the impact and after rebound as the elastic modulus and degree of plastic deformation are strong functions of temperature as shown in Fig. 2. In Fig. 3, the equivalent plastic strains and temperature profiles are compared for a series of initial particle temperatures varying from $T_i = 248$ to 348 K. The substrate temperature was held constant at $T_s = 298$ K for all cases.

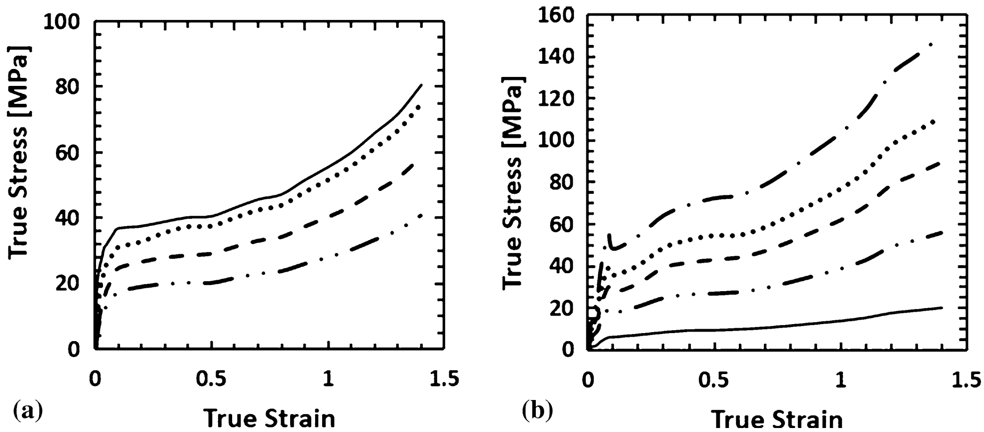

Fig. 2 Material properties of high-density polyethylene used as input into the von Mises model to simulate the particle impact. The data include (a) stress vs. strain at a constant temperature of $T_i = 298$ K and strain rates varying from (dashed double dotted line) $\dot{\varepsilon} = 0.0001\ s^{-1}$, (dashed line) $\dot{\varepsilon} = 0.01\ s^{-1}$, (dotted line) $\dot{\varepsilon} = 100\ s^{-1}$, (solid line) $\dot{\varepsilon} = 2460\ s^{-1}$ and (b) stress vs. strain at a constant strain rate of $\dot{\varepsilon} = 0.01\ s^{-1}$ and temperatures varying from (dashed single dotted line) $T_i = 198$ K, (dotted line) $T_i = 233$ K, (dashed line) $T_i = 293$ K, (dashed double dotted line) $T_i = 323$ K, (solid line) $T_i = 373$ K

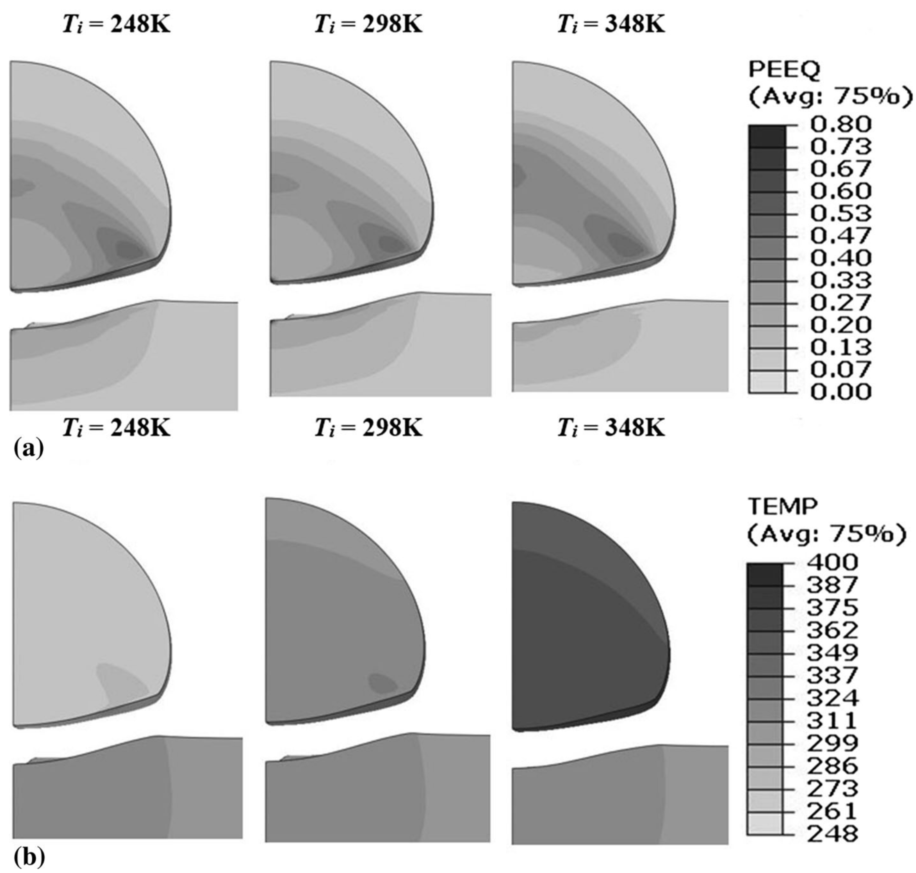

Fig. 3 Simulation results of the final deformed state of a 50 μm diameter high-density polyethylene particle impacting on a high-density polyethylene substrate at a temperature $T_s = 298$ K with an initial velocity $U_i = 200$ m/s. The particles shown have an initial temperature $T_i = 248$, 298 and 348 K. Data for (a) plastic deformation (PEEQ) and (b) temperature are shown

The particle velocity was held constant at $U_i = 200$ m/s as shown in Fig. 3.

In the simulations, the particle is released 5 μm away from the surface traveling at the impact velocity. The initial contact occurs along the vertical axis at the bottom of the particle. A large pressure is produced at impact, and it deforms the particle elastically and plastically. The elastic deformation results in energy stored in the particle which is recovered following the impact resulting in a finite rebound velocity U_r, and rebound kinetic energy, $KE_r = 1/2 m_p U_r^2$. We will utilize the rebound kinetic energy trends with parameter variations to better understand particle adhesion.

The plastic deformation of the particle results in non-recoverable particle substrate deformation and a rise in temperature at the particle and substrate interface. Plastic deformation will be analyzed by plotting maximum strain values in the particle and substrate, as well as the compression ratio of the particles, $C_r = (D_i - D_f)/D_i$, where D_i is the initial diameter of the particle and D_f is the final compressed height of the particle. In the sections that follow, we will present figures showing contours of both plastic equivalent strain and temperature for both the particles and substrate after impact. In the simulations, adhesion is not accounted for so the particles will always rebound after impact. The images are a few time steps after rebound. We will also present graphs showing trends in strain, temperature, rebound velocity and kinetic energy as well as compression ratio with varying input parameters.

As shown in Fig. 3(a) and graphs in Fig. 4(a), the localized maximum strains induced in the particle at various initial temperatures were almost identical. However, when compared to the low-temperature case, $T_i = 248$ K, the particle as a whole was subjected to larger average plastic strains with increasing temperature. This can be seen as an increase in the compression ratio with initial particle temperature in Fig. 4(d) from $C_r = 0.19$ to 0.23. The opposite trends were observed in the substrate as shown in Fig. 4(a). This is likely because the temperature and material properties of the substrate are fixed at $T_s = 298$ K. As a result, an increase in initial temperature of the particle results in the relevant softening of the particle compared to the substrate as shown in Fig. 2 which in turn leads to larger average strains throughout the particle with increasing particle temperature at the expense of the highly localized strain at the particle substrate interface. Small spikes of high temperatures were observed in the particle near the edge of the impact zone where the shear deformation is maximum; however, most of the

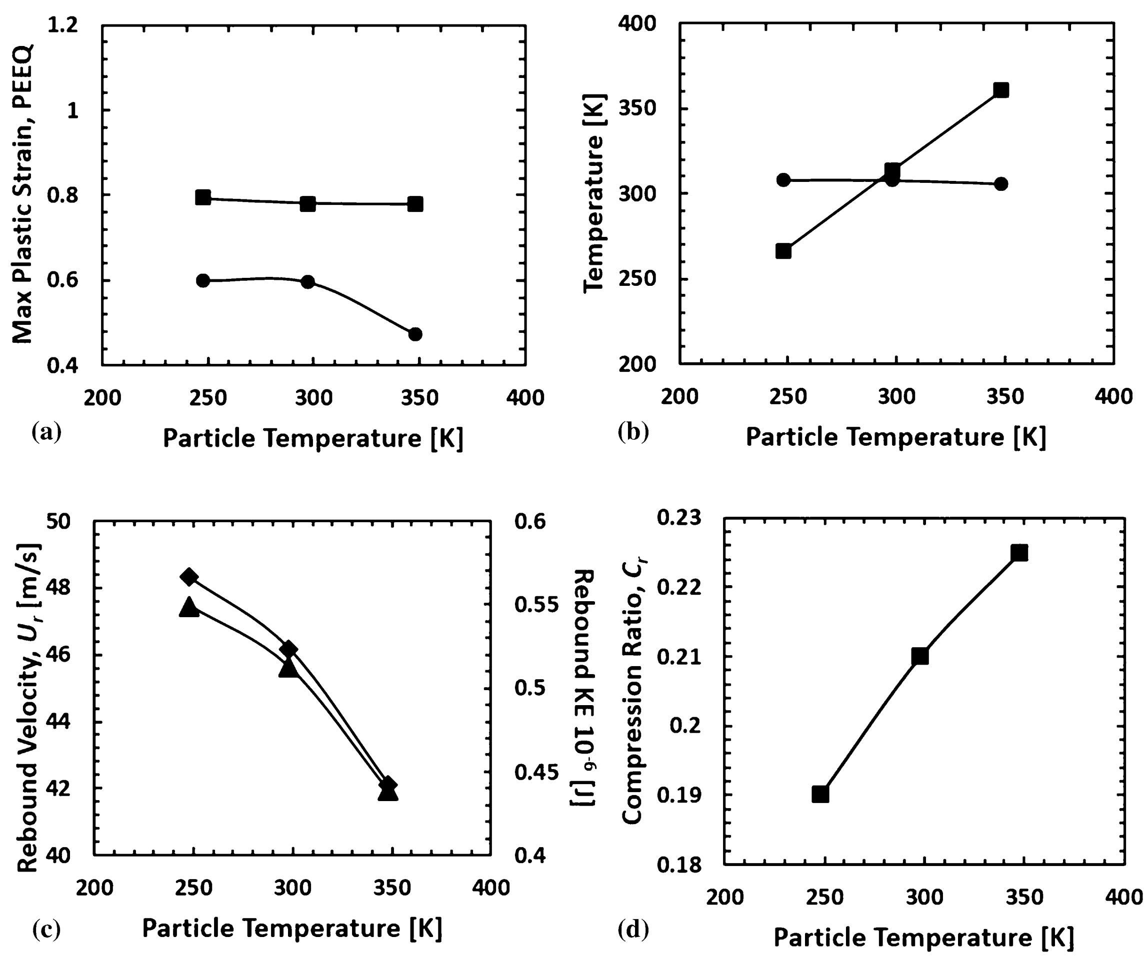

Fig. 4 Data showing the effect of initial particle temperature on: (a) maximum plastic deformation (PEEQ) in the (filled square) particle and (filled circle) substrate, (b) maximum temperature in the (filled square) particle and (filled circle) substrate, (c) (filled triangle) rebound velocity of the particle after impact and (filled diamond) rebound kinetic energy of the particle after impact, (d) (filled square) the compression ratio C_r of the particle. The simulations were carried on with an initial velocity of $U_i = 200$ m/s and initial temperature $T_i = 248$, 298 and 348 K for 50 μm particle diameter

temperature rise in the particle observed in Fig. 3(b) and 4(b) can be attributed to the increase in the initial particle temperature. As shown in Fig. 4(c), the rebound velocity and the rebound kinetic energy of the particle were reduced by 14 and 21%, respectively, as the temperature was increased from 248 to 348 K. These results suggest that the increase in particle temperature and its resulting softening might prove beneficial for particle adhesion even without accounting for the increase in chain mobility and entanglement during impact that will most likely enhance adhesion as the temperature rises.

To better understand whether the particles will likely adhere to the surface, we can compare the rebound kinetic energy, KE_r directly to the work of adhesion which is defined as

$$W_{PS} = (\gamma_P + \gamma_S - \gamma_{PS})A, \quad \text{(Eq 4)}$$

where A is the contact surface area between the particle and the substrate, γ_P is the surface tension of the particle, γ_S is the surface tension of the substrate and γ_{PS} is the interfacial tension between the particle and the substrate (Ref 20). The interfacial tension between the particle and the substrate can be estimated as

$$\gamma_{PS} = \gamma_P + \gamma_S - 2\sqrt{\gamma_P\gamma_S}. \quad \text{(Eq 5)}$$

The resulting work of adhesion becomes

$$W_{PS} = 2A\sqrt{\gamma_P\gamma_S}. \quad \text{(Eq 6)}$$

For impact of HDPE particle on HDPE substrate, $W_{PS} = 2A\gamma_P$ where $\gamma_P = 35.7$ mN/m (Ref 21). For the impact shown in Fig. 3, $W_{PS} = 0.9$ nJ. When compared against the rebound kinetic energy, KE_r shown in Fig. 4, the work of adhesion is two orders of magnitude too small to result in particle adhesion. Clearly, additional physics is needed to fully predict adhesion.

Effect of Initial Particle Velocity

As mentioned earlier, the impact behavior of the particle largely depends on the initial kinetic energy, thus the initial particle velocity. To understand the effect of the initial of particle velocity, the particle was impacted with initial velocity between $U_i = 150$ and 250 m/s. The equivalent plastic strain (PEEQ) and the maximum temperature distribution in the particle and the substrate just after the rebound of the particle for initial particle velocities of $U_i = 150$ to 250 m/s are shown in Fig. 5. For the range of velocities tested, the plastic deformation and the temperature of the material were found to increase with increasing particle velocity. It is evident from Fig. 5 that the

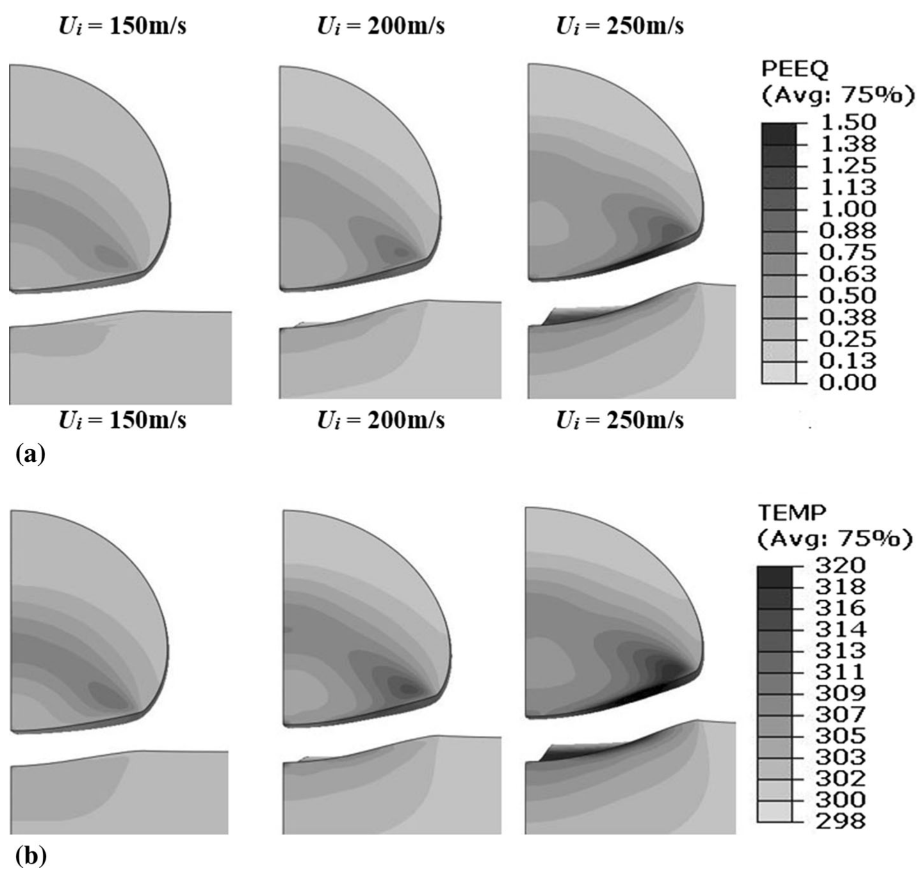

Fig. 5 Simulation results of the final deformed state of a 50 μm diameter high-density polyethylene particle impacting on a high-density polyethylene substrate at an initial temperature $T_i = 298$ K. The particles shown have an initial velocity $U_i = 150$, 200 and 250 m/s. Data for (a) plastic deformation (PEEQ) and (b) temperature are shown

equivalent plastic strains increased by almost 300% for a 100 m/s increase in initial velocity of the particle. The highest deformations were confined to volumes at the particle substrate interface resulting in a significant increase in the temperature in these regions from $T_{\max} = 305$ K at 150 m/s to $T_{\max} = 320$ K at 250 m/s. As the particle velocity was increased, the particle formed an increasing deep crater into the substrate. In order to quantify the particle deformation, the compression ratio or the flattening ratio is defined as the ratio of the change in particle diameter to the initial particle diameter, $C_r = (D_i - D_f)/D_i$. The compression ratio was found to increase from $C_r = 0.15$ to 0.25 with increasing particle velocity suggesting higher average strains in the particles with higher impact velocity as shown in Fig. 6(d). The model does not account for material melting due to temperature rise. Therefore, the energy that should have been utilized for the phase change appears in the form of large temperature spikes at the particle substrate interface where the melting is assumed to take place. Given the high speeds and the impact duration which can last <100 ns, neglecting melting which can take seconds or minutes may be a reasonable assumption. No visible jetting is observed for velocities as high as 250 m/s. Further increase in the particle velocity causes excessive mesh distortion leading to convergence problems and thus was not included.

Effect of Particle Size

In previous numerical studies, mechanics of metal particle impact has been shown to strongly depend on the ratio of the kinetic energy per unit volume of the particle to the plastic strain energy density (Ref 1, 22). This non-dimensional parameter is expressed as $\rho U_i^2/\sigma_Y$, where ρ and U_i are particle density and velocity, respectively, and σ_Y is the substrate's dynamic yield strength. Thus, from the above relation, the results are expected to be independent of the particle diameter if the material behavior is rate

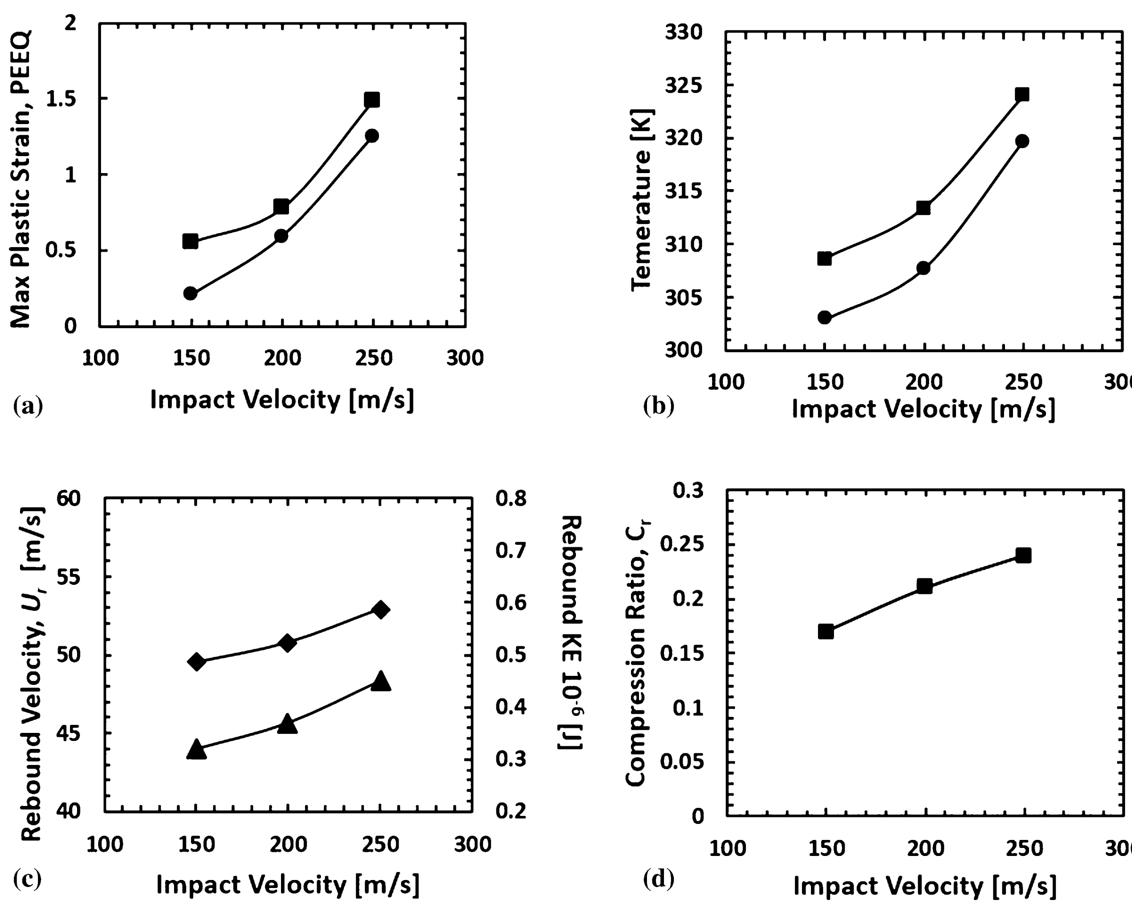

Fig. 6 Data showing the effect of initial particle velocity on: (a) maximum plastic deformation (PEEQ) in the (filled square) particle and (filled circle) substrate, (b) maximum temperature in the (filled square) particle and (filled circle) substrate, (c) (filled triangle) rebound velocity of the particle after impact and (filled diamond) rebound kinetic energy of the particle after impact and (d) (filled square) compression ratio C_r of the particle. The simulations were carried on with an initial velocity of $U_i = 150$, 200, 250 m/s and initial temperature $T_i = 298$ K for 50 µm particle diameter

independent and the gravitational effects are negligible. Since we are dealing with micron-sized bodies, the gravitational effects can be considered negligible. However, as shown in Fig. 2(a), the material behavior is highly rate dependent, and thus, the effect of particle size needs to be investigated.

In order to study the effect of HDPE particle size, impact of particles with diameter of 50, 250 and 500 μm was simulated on an HDPE substrate for an initial particle velocity of $U_i = 200$ m/s. The contours of plastic deformation and temperature distribution in the particle and substrate are shown in Fig. 7. Although the particle diameter was increased by a factor of 10 and the impact kinetic energy by 1000, little change in the strain field or the temperature profile was observed with increasing particle size. In Fig. 8(d), the compression ratio C_r which can be viewed as average deformation of the particle is plotted as a function of the particle size. A monotonic growth in the compression ratio of 15% was observed with increasing particle size even as both the maximum temperatures and strains were found to demonstrate very little change as shown in Fig. 8(c) and (d). Smaller particles tend to act stiffer than larger particles due to the higher strain rates and thus higher dynamic yield strength they encounter during impact. Thus, our simulations clearly show that it is easier to deform larger particles upon impact. Adhesion, however, was found to trend very differently. The rebound velocity and the corresponding rebound kinetic energy are plotted in Fig. 8(c) for varying particle diameter. The rebound particle velocity was found to reduce with increasing particle size due to increase in the average strain observed in the compression ratio. The rebound kinetic energy was found to increase with particle size due to the increase in the mass of the particle. If the particle rebound kinetic energy KE_r is normalized by the particle mass, the data in Fig. 8 would demonstrate that more of the incoming kinetic energy is dissipated as thermal energy during impact of larger particles due to the larger plastic deformation of the particle. Unfortunately, even as more kinetic energy was dissipated for larger diameter particles, the rebound kinetic energy KE_r will grow like the mass of the particle or its volume $KE \propto D^3$, while the work of adhesion will grow with the cross-sectional area, $W_{PS} \propto D^2$. As a result,

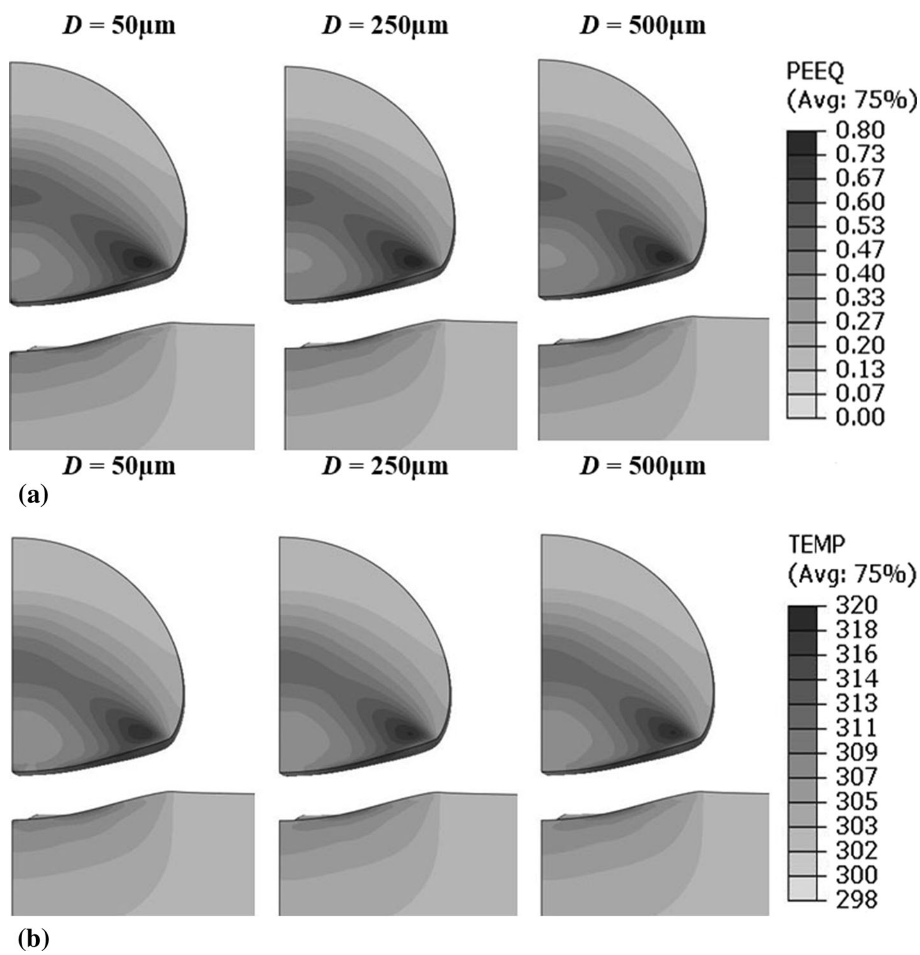

Fig. 7 Simulation results showing the final deformed state of high-density polyethylene particle impacting on a high-density polyethylene substrate at $U_i = 200$ m/s and initial temperature $T_i = 298$ K with particle diameter D varying from $D = 50$ to 500 μm. In (a), the plastic deformation (PEEQ) and (b) the temperature variation is shown

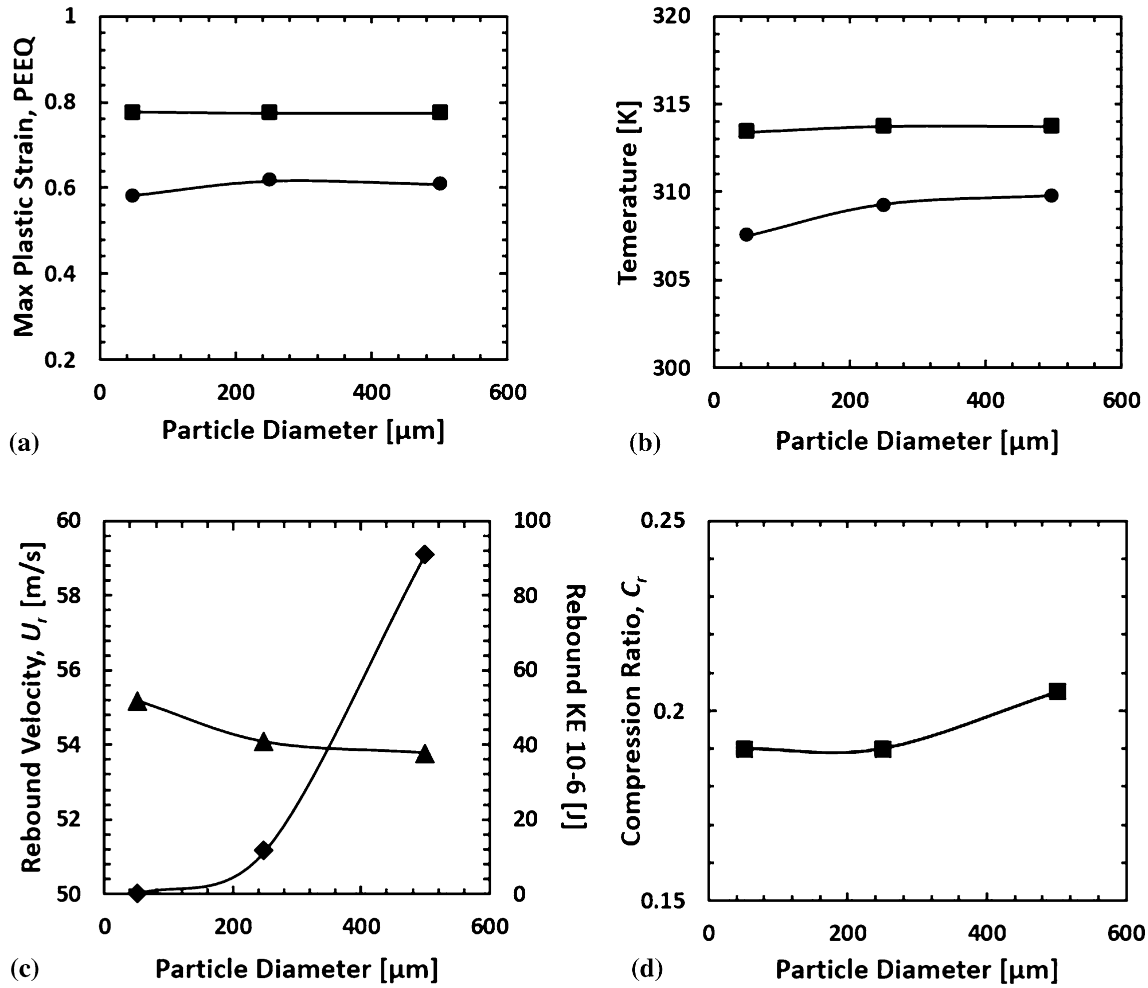

Fig. 8 Data showing the effect of particle diameter D on: (a) maximum plastic deformation (PEEQ) in the (filled square) particle and (filled circle) substrate, (b) maximum temperature in the (filled square) particle and (filled circle) substrate, (c) (filled triangle) rebound velocity of the particle after impact and (filled diamond) rebound kinetic energy of the particle after impact, (d) (filled square) compression ratio, C_r of the particle. The simulations were carried on with an initial velocity of $U_i = 200$ m/s and initial temperature $T_i = 298$ K

unless the rate-dependent material properties result in a rebound kinetic energy that grows slower than D^2, smaller particles will always be expected to adhere more strongly on impact.

Effect of Substrate Material Hardness

As described earlier, the effectiveness of adhesion of the particle depends on the difference between the rebound kinetic energy and the work of adhesion W_{ps} between the particle and the substrate. The work of adhesion is a direct function of the contact surface area A between the particle and the substrate and also the surface tension (γ_P and γ_S) of the particle and substrate material. Changing the particle or the substrate can affect the surface tension. Additionally, the contact area is directly related to the relative hardness between the particle and the substrate. Thus, depending on how hard the substrate is compared to the particle, the surface area generated during the impact will change. The larger the deformation, the larger the work of adhesion and the less elastic strain energy stored in the particle and the substrate returning to the particle as rebound energy.

To study the effect of substrate hardness, four different substrate materials were chosen: LDPE, HDPE, PC and OFHC copper. In each case, a 50-μm-diameter HDPE particle was used to impact the substrate with an impact velocity of $U_i = 200$ m/s.

As the substrate was changed from LDPE to HDPE to PC and finally to copper, the modulus was increased from $E = 0.3$ to 1.26 GPa. It can be observed from Fig. 9 that with increasing substrate modulus, the particle tended to

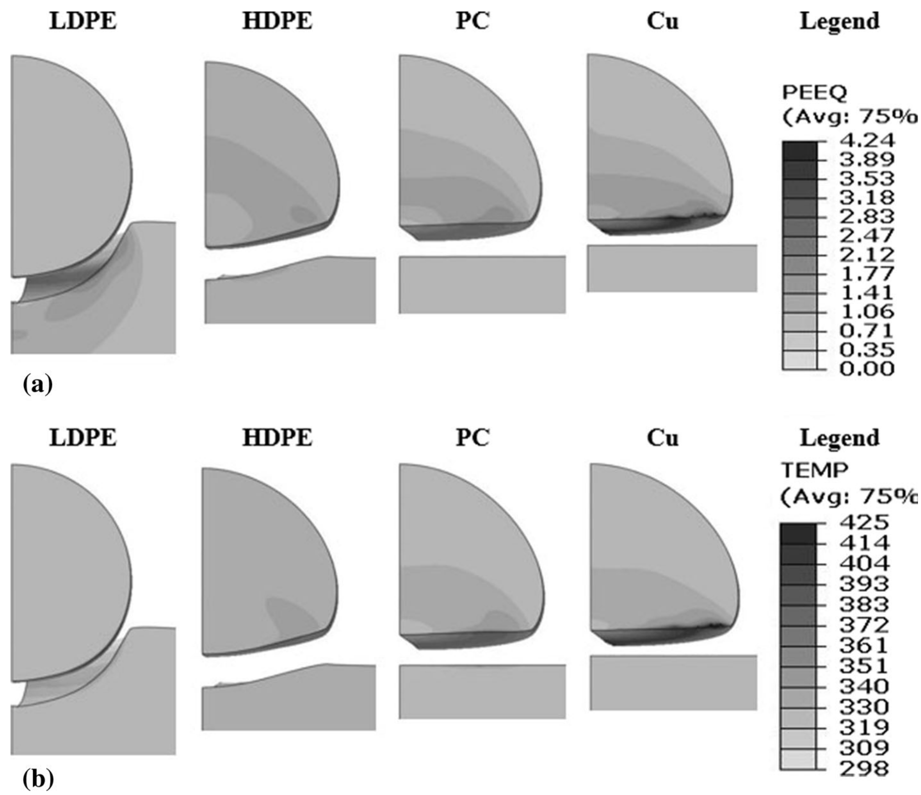

Fig. 9 Simulation results showing the final deformed state of a 50 μm diameter high-density polyethylene particle on a low-density polyethylene (LDPE) substrate, high-density polyethylene (HDPE) substrate, polycarbonate (PC) substrate and Cu substrate with initial velocity $U_{\mathrm{i}} = 200$ m/s and initial temperature $T_{\mathrm{i}} = 298$ K. (a) The plastic deformation (PEEQ) and (b) the temperature distribution are shown

spread laterally, while simultaneously, the depth of the crater in the substrate was reduced. Interestingly, the HDPE/HDPE case resulted in the minimum temperature and plastic strain while producing the maximum rebound kinetic energy and velocity. With mismatch in modulus, the strain is disproportionately distributed to the softer particle/substrate. The result is more plastic deformation in the softer of the two elements and more energy dissipation. As seen from the results presented in Fig. 10, the plastic deformation and temperature distribution in the particle increased as the substrate modulus increased, while the opposite trend was observed in the substrate. For impact on copper substrate, a compression ratio of $C_{\mathrm{r}} = 0.3$ was observed with no plastic deformation of the substrate. For a substrate with a lower modulus than the particle, HDPE/LDPE case, the particle barely deformed, $C_{\mathrm{r}} = 0.05$, while the substrate experienced a large plastic deformation with PEEQ = 3. Thus, from the standpoint of rebound kinetic energy only, the like-on-like deposition is the most difficult to achieve. This phenomenon has also been observed experimentally by Bush et al. (Ref 9). Additional effects like local polymer melting and entanglement which could enhance adhesion are not accounted for here. Thus, even though the particle experiences great deformation and local heating during impact on copper, it may not adhere as easily as on the polycarbonate for example.

Effect of Substrate Coating Thickness

As explained in the previous section, the substrate properties can have significant effect on the rebound characteristics of the particle. Experiments have shown that deposition on a cold metal substrate is challenging even though the modulus mismatch reduces the rebound kinetic energy (Ref 12). This is because deposition onto a non-polymeric substrate must rely on the work of adhesion alone without the benefit of polymer entanglement. In order to work around this problem, one could imagine applying a precoating of polymer to a metal surface prior to cold-spray deposition. This approach will take advantage of the mismatch in modulus while also allowing for polymer entanglement and bonding. In this section, we investigate the effect of an existing layer of coating on the deformed shape of the particle and the rebound characteristics. For this case, an HDPE particle is used to impact on a hard copper substrate with a thin coating of HDPE with the same material properties as the impacting particle. The coating thickness was varied from 2.5 to 250 μm coating. Beyond 100 μm, the results were equivalent to an infinitely thick HDPE film/substrate.

The particle shape after impact along with the contours of the plastic deformation and temperature distribution in the particle and the coating is shown in Fig. 11. For

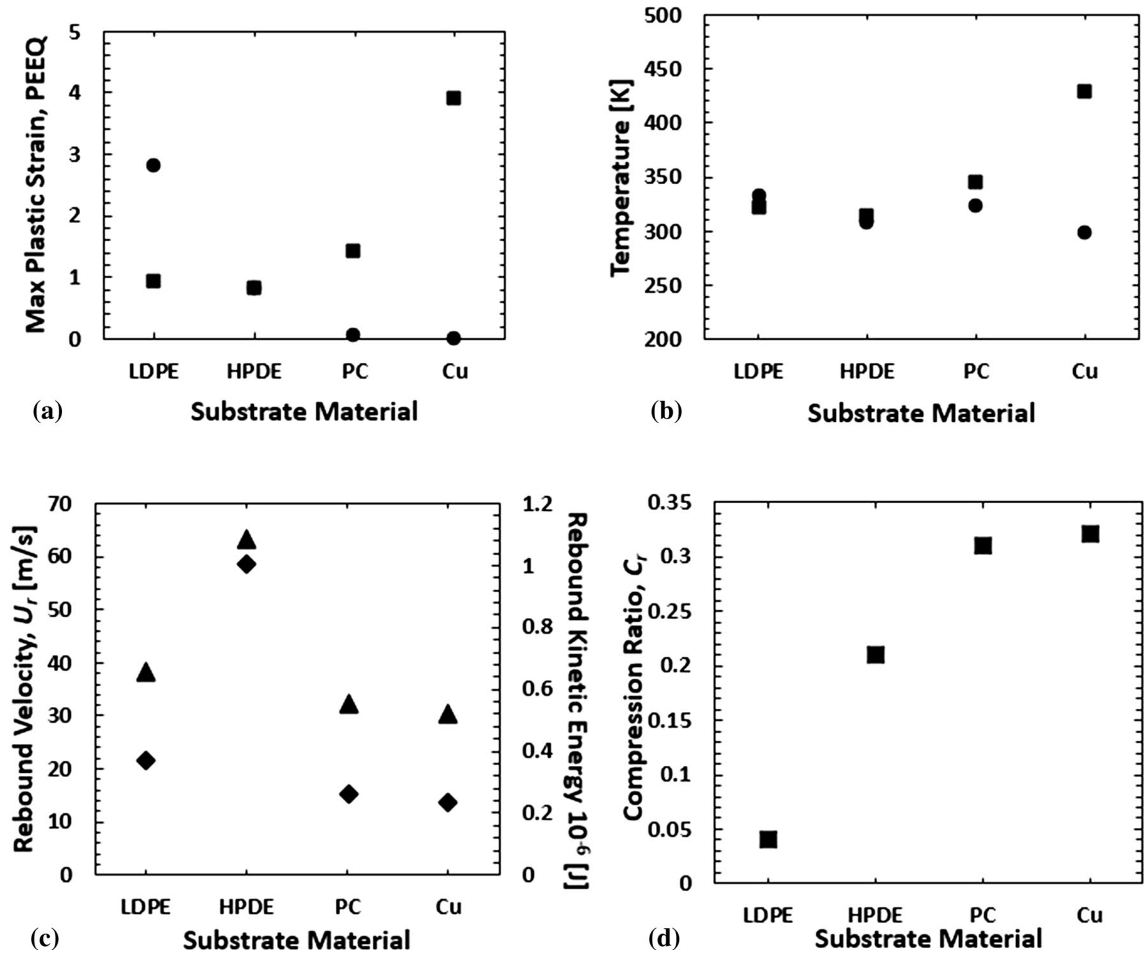

Fig. 10 Data showing the effect of substrate hardness on: (a) maximum plastic deformation (PEEQ) in the (filled square) particle and (filled circle) substrate, (b) maximum temperature in the (filled square) particle and (filled circle) substrate, (c) (filled triangle) rebound velocity of the particle after impact and (filled diamond) rebound kinetic energy of the particle after impact and (d) (filled square) compression ratio C_r of the particle. The simulations were carried on with an initial velocity of $U_i = 200$ m/s and initial temperature $T_i = 298$ K for 50 µm particle diameter

comparison, the value for HDPE particle impact on copper substrate is shown in Fig. 10 and is included in Fig. 12 for comparison. The effect of coating thickness on particle rebound velocity and rebound kinetic energy is shown in Fig. 12(c). Although the maximum plastic strains in the particle and substrate with a thin 2.5 µm HDPE coating were half as much as impacts on pure Cu substrate, the compression ratio of the particle only changed by a few percent and due to the plastic deformation of the substrate; a 15% reduction in the rebound velocity was observed. For 5-20 µm-thick coatings, a rebound velocity comparable to pure copper was observed. For thicknesses beyond 20 µm, an increase in the rebound velocity toward the result for pure HDPE was found. This reduction in the velocity can be attributed to the large deformations in the particle and plastic deformations produced in the thin film coating as shown in Fig. 11. Enormous shear stresses and deformation were introduced into the thin film upon impact. This energy was dissipated in the form of a temperature rise due to plastic deformation in the particle and the coating. Higher deformation leads to increased temperatures, more polymer mobility and more entanglement between the polymer in the substrate and the polymer in the particle. A thin layer of polymer is often needed especially on inorganic substrates to improve deposition because without that thin layer polymer entanglement is not possible and one must rely on the work of adhesion alone. As shown in "Effect of Particle Temperature" section, work of adhesion does not appear to be large enough in most cases to achieve deposition. For a coating thickness <20 µm, the particle with a velocity of 200 m/s had enough energy to plastically deform the entire thickness of the coating. The hard copper substrate beneath the coating further amplifies the plastic deformation of the coating by three times compared to infinitely thick HDPE/

Fig. 11 Simulation results showing the final deformed state of a 50 μm diameter high-density polyethylene particle impact on a copper substrate with a coating thickness $t = 2.5$, 20 and 100 μm with initial velocity $U_i = 200$ m/s and initial temperature $T_i = 298$ K. (a) Particle deformation (PEEQ) and (b) the temperature distribution are shown

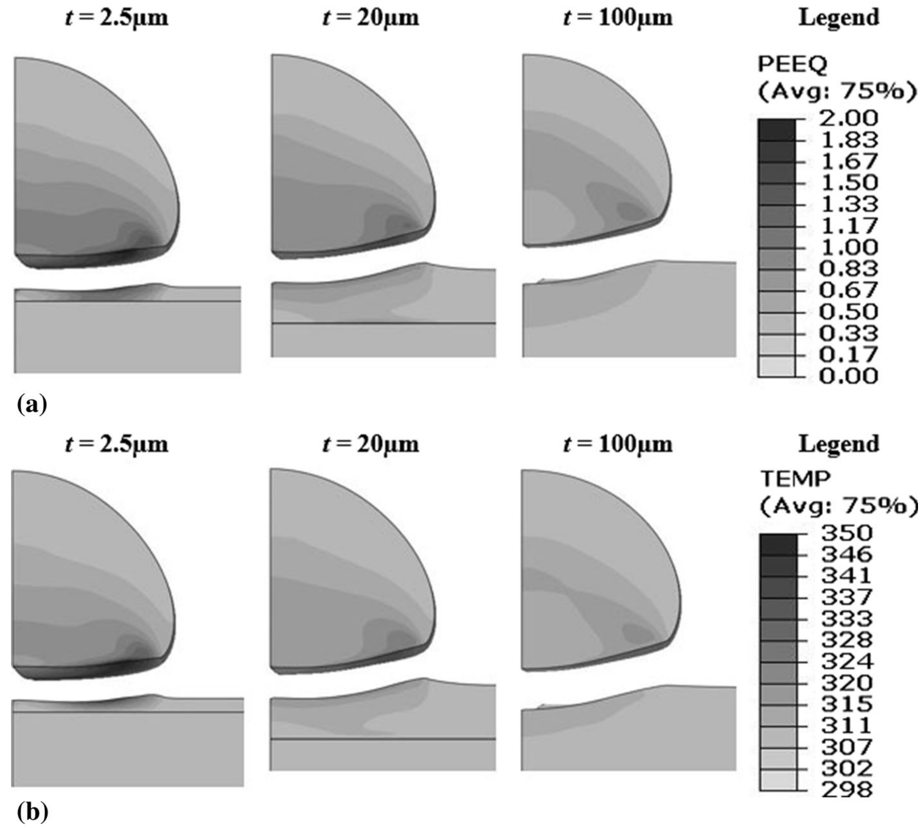

HDPE case, thus generating a large shear stress in the coating during impact. Once the thickness becomes more than 20 μm, the effect of the underlying Cu substrate reduces. Thus, it is clear that having a very thin coating of the softer or similar material will improve deposition on a hard non-polymer substrate. This could be useful for practical applications where a thin coating can be added to aid adhesion for the succeeding layers. The current model can also be used as the first step for multiple particle impacts where this first particle adhesion may be challenging, but will likely become easier once an initial coating has formed.

Summary and Conclusions

In the study presented here, the impact of a single polyethylene particle on a variety of polymeric and inorganic substrates was carried out using the von Mises plasticity model with strain-rate and temperature-dependent material properties data obtained from the literature (Ref 15). The impact of a 50 μm diameter particle was studied over a wide range of impact temperatures, impact velocities, diameter and onto a range of substrates with different material properties to better understand the impact dynamics of polymeric particles.

In the simulations presented here, as the particle impacted the substrate, a large pressure was produced at the impact location which deformed the particle both elastically and plastically. The elastic deformations were stored as recoverable elastic energy which was recovered following the impact in a finite rebound velocity and rebound kinetic energy. The plastic deformation dissipated energy causing the temperature to rise and the rebound velocity to drop. The result of the impact on the particle and substrate was analyzed by plotting the maximum plastic strains and the temperature profiles as a function of changing initial conditions and particle/substrate composition. The average deformation in the particle was also presented in terms of the compression ratio.

The effect of initial particle temperature was studied while varying the initial temperature of the particle from $T_i = 248$ to 348 K and keeping the substrate temperature $T_s = 298$ K. The localized strains induced in the particle at various initial temperatures were almost identical. However, the particle as a whole was subjected to larger average strains with increasing temperature. This was most evident in the compression ratio, C_r. As the particle temperature was increased, the plastic deformation in the substrate decreased. This increased plastic deformation resulted in a drop of 14% in the rebound velocity and 21%

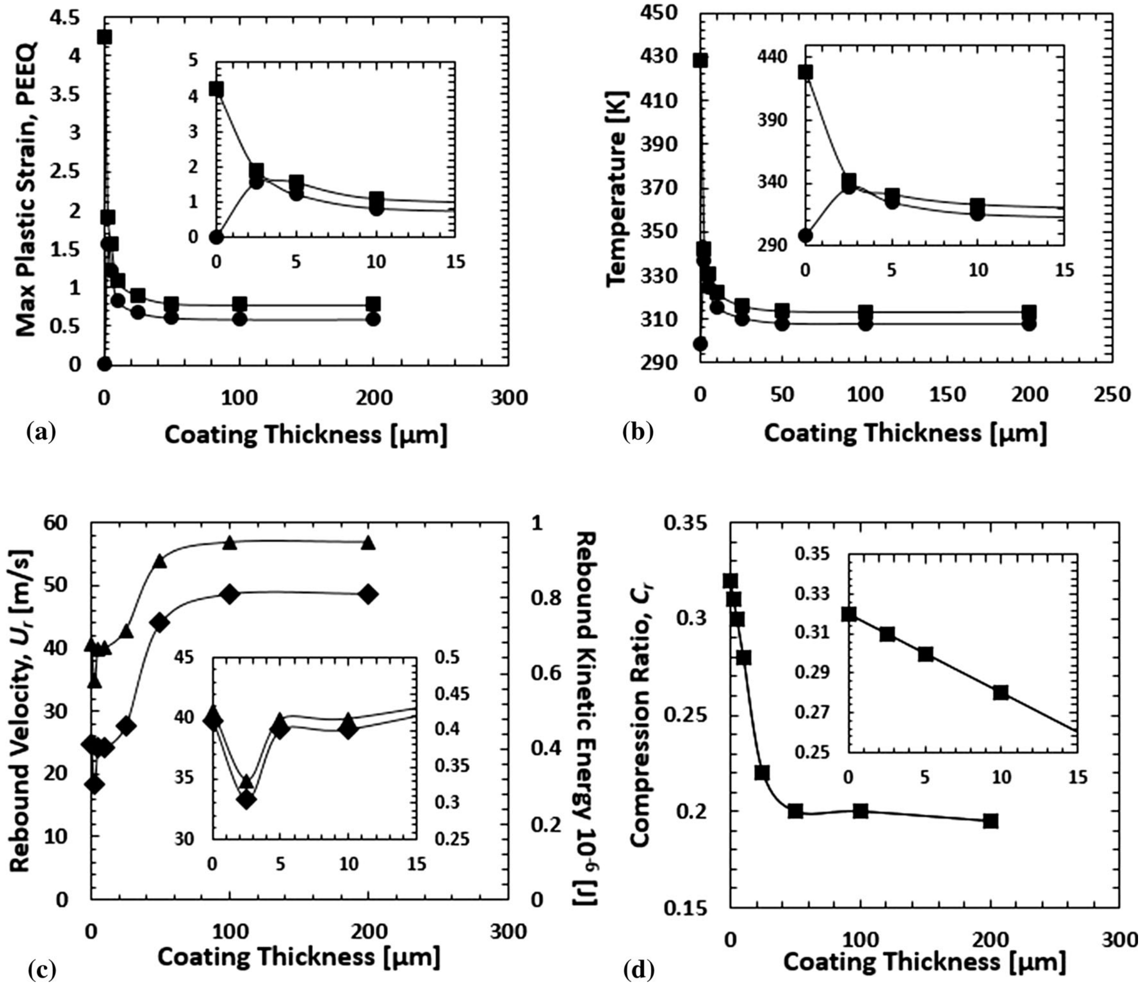

Fig. 12 Data showing the effect of thickness of high-density polyethylene coating on copper substrate on: (a) plastic deformation (PEEQ) in the (filled square) particle and (filled circle) coating, (b) temperature in the (filled square) particle and (filled circle) coating, (c) (filled triangle) rebound velocity of the particle after impact and (filled diamond) rebound kinetic energy of the particle after impact and (d) (filled square) compression ratio, C_r of the particle after impact. The simulations were carried on with an initial velocity of $U_i = 200$ m/s and initial temperature $T_i = 298$ K for 50 µm particle diameter

in the rebound kinetic energy with increasing temperature of the particles. Thus, increasing the particle temperature and its resulting softening would prove beneficial for particle adhesion. The initial particle velocity was found experimentally to play a great role in adhesion of the particle (Ref 12). Thus, the effect of particle velocity was studied by varying the impact velocity from $U_i = 150$ to 250 m/s. Increasing the initial particle velocity was found to greatly increase the plastic deformation in the particle. However, the rebound velocity and the rebound kinetic energy increased with the increasing initial velocity. Due to highly strain-rate-dependent behavior of polymers, the effect of particle size was also investigated. The particle diameter was varied from $D = 50$ to 500 µm and keeping the particle velocity $U_i = 200$ m/s and temperature $T_i = 298$ K. Particle diameter did not affect the particle deformation, temperature profiles or rebound velocity significantly. However, a monotonic growth in the compression ratio C_r was observed which indicated that the larger particle deformed easily. That being said, although rebound velocity was not found to change, the kinetic energy was found to grow like the mass of the particle or its volume, KE $\propto D^3$. With regard to the particle adhesion, this is a negative result because the work of adhesion grows with the contact area between the particle and the substrate, $W_{PS} \propto D^2$. As a result, smaller particles should always be expected to adhere more strongly than larger particles upon impact.

The substrate material was found to play an important role when it comes to adhesion of the particle because the relative hardness of the substrate is an important factor to consider. The effect of substrate hardness was studied by impacting an HDPE particle on four different substrate materials: LDPE, HDPE, PC and copper. The substrate strength increased from $E = 0.3$ to 1.26 GPa as the material was changed from LDPE to HDPE to PC and finally to copper. It was found that the best results were obtained when there was a mismatch between the particle and substrate material strength, resulting in either large plastic deformation in the particle for harder substrates or the substrates for softer substrates. Thus, a mismatch in the modulus proved to be beneficial for particle adhesion.

The effect of having a modulus mismatch was further exploited by simulating the impact of an HDPE particle on a hard copper substrate with a thin HDPE film. The simulations were carried with an HDPE particle impacting the copper substrate with a thin film and varying the film thickness from $t = 2.5$ to 250 µm. Although the plastic strains in the particle and substrate for a 2.5 µm thin film were only 50% when compared to no film (impact on copper substrate), the rebound velocity was found to reduce by 15%. This reduction was due to the large deformations in the particle and the plastic deformations produced in the thin film coating which led to the development of enormous shear stresses. Thus, most of the particle energy was dissipated in the form of plastic deformation and temperature rise in the particle and the thin film. This effect diminished as the coating thickness approached $t = 20$ µm, beyond $t = 20$ µm the particle behaved as if impacting on an infinite HDPE substrate. Thus, having a very thin coating of a softer or similar material will improve deposition on a hard non-polymer substrate.

Although these results give satisfactory insight about the impact dynamics of polymers and the various factors affecting the impact behavior, the current model still lacks to account for many phenomena such as melting of the material, adhesion of the particle to the substrate and polymer chain interactions and entanglements between the particle and the substrate. More advanced models that can account for these phenomena and give better predictions for polymer particle impact are still needed if quantitative predictions of experimental results are to be achieved.

References

1. B. Yildirim, S. Muftu, and A. Gouldstone, Modeling of High Velocity Impact of Spherical Particles, *Wear*, 2011, **2011**(270), p 703-713
2. J.A. Zukas, *High-Velocity Impact Dynamics*, Wiley, Hoboken, 1990
3. ARL, *Centre for Cold Spray Cold Spray Process.* Retrieved 1 April 2014, from http://www.arl.army.mil/www/default.cfm?page=370, 2010.
4. H. Assadi, F. Gärtner, T. Stoltenhoff, and H. Kreye, Bonding Mechanism in Cold Gas Spraying, *Acta Mater.*, 2003, **51**(2003), p 4379
5. T. Hussain, D.G. McCartney, P.H. Shipway, and D. Zhang, Bonding Mechanism in Cold Spraying: The Contribution of Metallurgical and Mechanical Components, *J. Therm. Spray Technol.*, 2009, **18**(3), p 364
6. T. Schmidt, F. Gärtner, H. Assadi, and H. Kreye, *Acta Mater.*, 2006, **54**(2006), p 729-742
7. W.-Y. Li and W. Gao, Some Aspects of 3D Numerical Modeling of High Velocity Impact of Particles in Cold Spraying by Explicit Finite Element Analysis, *Appl. Surf. Sci.*, 2009, **255**(2), p 7878-7892
8. X. Zhou, X. Wu, H. Guo, J. Wang, and J. Zhang, Deposition behavior of multi-particle impact in cold spraying process, *Int. J. Miner. Metall. Mater.*, 2010, **17**(5), p 635
9. T.P. Bush, Z. Khalikhali, V. Champagne, D. Schmidt, and J.P. Rothstein, Optimization of Cold-Spray Deposition of High Density Polyethylene Powders, *J. Therm. Spray Technol.*, 2017 (submitted)
10. K. Ravi, Y. Ichikawa, K. Ogawa, T. Deplancke, O. Lame, and J.-Y. Cavaille, Mechanistic Study and Characterization of Cold-Sprayed Ultra-high Molecular Weight Polyethylene-Nano-ceramic Composite Coating, *J. Therm. Spray Technol.*, 2015, **25**(1-2), p 160-169
11. N. Sanpo, M.L. Tan, P. Cheang, and K.A. Khor, Antibacterial Property of Cold-Sprayed HA-Ag/PEEQ Coating, *J. Therm. Spray Technol.*, 2008, **18**(1), p 10-15
12. Y. Xu and I.M. Hutchings, Cold Spray Deposition of Thermoplastic Powder, *Surf. Coat. Technol.*, 2006, **201**, p 3044-3050
13. V.K. Champagne, *The Cold Spray Materials Deposition Process: Fundamentals and Applications*, Woodhead Publishing, Cambridge, 2007
14. ABAQUS, *Academic Research User Manual Guide* (In Release 6.14)
15. M. Dean, *Determination of Material Properties and Parameters Required for the Simulation of Impact Performance of Plastics Using Finite Element Analysis*, 2004
16. N.P. Laboratory, *Manual for the Calculation of Elastic Plastic Material Model Parameters*, 2007
17. J.S. Inc, *Material Properties Database, MPDB*
18. J. Richeton, S. Ahzi, K.S. Vecchio, F.C. Jiang, and R.R. Adharapurapu, *J. Solids Struct.*, 2006, **43**, p 2318-2335
19. Y. Gnanou and M. Fontanille, *Organic and Physical Chemistry of Polymers*, Wiley, Hoboken, 2008, p 13-18
20. J. Israelachvili, *Intermolecular and Surface Forces*, 2nd ed., Academic Press, Cambridge, 1991 (An Elsevier Science Imprint)
21. F.M. Fowkes, *Ind. Chem. Eng.*, 1964, **56**, p 40
22. K.L. Johnson, *Contact Mechanics*, Cambridge University Press, Cambridge, 1985